Rotor Optimization for Synchronous Reluctance Motors

Ken Chen, Wenfei Yu, and Chuanxin Wen

***Abstract* — Rotor of Synchronous reluctance motor (SynRM) usually has multiple flux barrier structure for the purpose of higher electromagnetic torque and lower torque ripple. Two different strategies are used in this paper for rotor structure optimization and a compromised strategy for fully squeeze the potential of each related parameters is developed. Performance of resulted rotor structure is evaluated to verify the optimization procedure.**

***Index Terms*—Finite element analysis, maximum torque, optimization strategy, rotor structure, synchronous reluctance motor, torque ripple.**

I. Introduction

THE concept of synchronous reluctance machines (SynRMs) has been proposed decades ago, which produces electromagnetic torque only by inductances difference between direct-axis (*d*-axis) and quadratic-axis (*q*-axis) due to its specific rotor structure [1]. With no rare-earth permanent magnets (PMs)[1] or windings on its rotor, the SynRM can have relatively lower cost, more robust structure and higher efficiency [2]. These advantages lead a rapid raise of research interests of SynRMs in recent years [3], which considers SynRM as a suitable alternative for induction motors (IMs) and a potential opponent for PM synchronous motors (PMSMs).

Since SynRM has similar stator structure compared with other type of motors, e.g., IMs and PMSMs, most SynRM designs focus on the rotor structure part. ALA (Axially Laminated Anisotropic) and TLA (Transversally Laminated Anisotropic) are the two main-stream rotor design schemes for SynRMs [4]. The ALA rotor is produced by alternatively stacking lamination layers and insulation layers on its axial direction. Although its high salient ratio can result a good performance in torque and power factor, industrial application of ALA rotor is still quite limited due to its complex producing procedure and low mechanical strength [3]. On the other hand, the TLA rotor is produced by processing air barriers on silicon steel plates and stacking those pieces through the shaft. It has slightly weaker performance than the ALA rotor, but much simpler manufacture process and stronger mechanical strength [5]. Due to these considerations, the optimization will be based on the TLA rotor type.

For the specific SynRM rotor structure, increasing flux barrier number will achieve higher salient ratio and thus higher electromagnetic torque and higher power factor [6]. However, increasing the number of flux barriers will also greatly increase the design dimensions and thus create heavy load for the optimization [7].

The purpose of this paper is using two-dimensional finite element method (2D-FEM) to investigate a strategy to fast design and optimize a rotor structure of SynRMs. The optimization result will also be evaluated by critical parameters of the machine performance.

II. Optimization Strategy

Optimization of the SynRM rotor structure is aiming to obtain higher electromagnetic torque, smoother torque output with lower torque ripple, lower core loss and higher power factor. For convenience, the average torque and torque ripple are selected as the indicators in the design process.

A. Different Optimization Approaches

General optimization procedure prefers to optimize selected parameters once a time and summarize values of the best points for the final design. This type of strategy has advantages on modifying the number of parameters, increasing precision for better value, identifying best case from data and changing test range for optimizing parameters. Using this strategy to optimize one rotor structure can be fast and easy. Taking Svetlana's method as example, the author picked four parameters, optimized their values and combined the results for the final set value of the design [8]. The paper takes only 22 simulations to finish the optimization. However, consider those parameters are depend with each other and will have co-effect on overall magnetic paths, it is very unlikely to achieve global optimal with this single optimization procedure.

Another type of optimization strategy tests all possible sets of value for selected parameters and tries to find the best set of values. This strategy can definitely achieve global optimal, but it also has some shortages that cannot be ignored, e.g., time consuming and precision limitation. Taking Crisian's method as an example, the author selected four parameters for the optimization and compared about 3200 cases to find the best

Manuscript was submitted for review on 27, September, 2018.

Ken Chen received the B.S. degree in Electrical Engineering from Purdue University, West Lafayette, USA, in 2017 and currently working toward M.S. degree in Electrical Engineering in Ming Hsieh Department of Electrical engineering, University of Southern California, Los Angeles, USA. (e-mail: kenc@usc.edu)

Wenfei Yu received the M.S. degree in electric machines at Zhengzhou University of Light Industry, Zhengzhou, China, in 2018. Since 2018, he has been working toward the Ph.D. degree in the School of Electric Eengineering, Southeast University, Nanjing, China.

Chuanxin Wen received the M.S. Degrees in Electrical engineering from Southeast University, Nanjing, China, in 2004. Since 2004, he has been with NARI Group Corporation, where he is currently a manager of electric vehicle drive system.

Digital Object Identifier 10.30941/CESTEMS.2019.00036

set of value [7]. Time for the whole procedure relies heavily on efficient calculation algorithm and powerful processors, which can vary between hours and months.

B. Combined Strategy

A combined, comprehensive optimization strategy of two mentioned methods is described in Fig. 1, which aims to fully squeeze potential of the rotor structure and shorter the time taken for the procedure. Detail procedure includes a rough optimization and several iterations of fine optimizations.

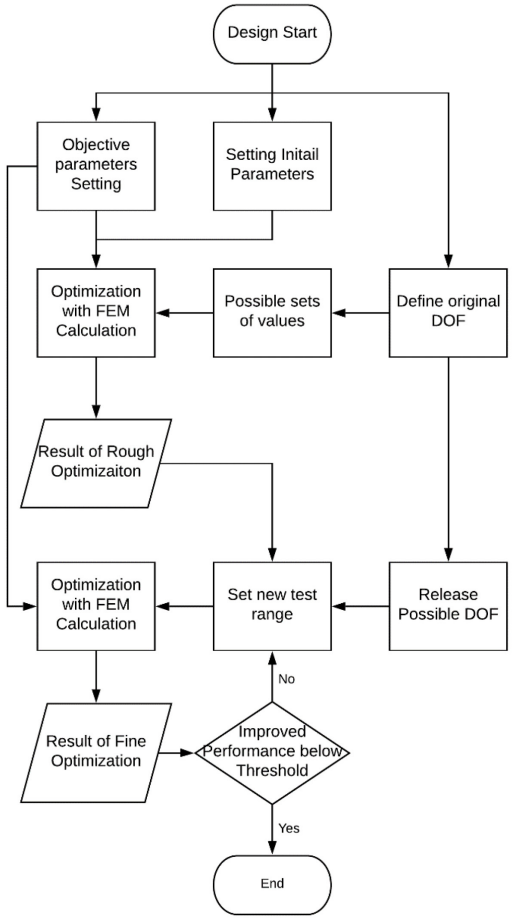

Fig 1. Detail procedure of the new combined optimization strategy.

A rough optimization includes assigning reasonable value to certain parameters, finding least essential parameters that can undoubtedly define the whole structure and testing possible sets of values for found parameters. Consider only few parameters are used to optimization (usually two or three), rough optimization won't take much time and can produce a rotor structure with considerable degree of completion. Then, the geometry of rotor is re-defined using a more specific way [9]. All possible degrees of freedoms (DOFs) of the model are released and their referenced values are calculated due to the values of the parameters from the rough optimization. After that, several iterations of the fine optimization will be proceeding to generate the final design. One iteration of fine optimization includes sequentially picking all released parameters, setting suitable test ranges from their reference values, testing and replacing the value if simulation proves improving in performance. Result from each iteration will be compared and the procedure will be stopped if the overall improving in performance is lower than a preset threshold.

The whole procedures can remove rough optimization and include only finding all possible DOFs and doing iterations of fine optimization, it just need more iterations and longer time to reach the same result.

III. Optimization

The optimization will focus on the rotor structure geometry and its corresponding stator's dimension is fixed. The parameters of the machine are listed in Table I.

TABLE I
MACHINE PARAMETERS

Parameter	Value	Parameter	Value
Pole-pair number	3	Slot number	45
Stator outer diameter	182.2mm	Stator inner diameter	127.2mm
Air gap	0.3mm	Stack length	90mm
Slot opening width	3mm	Slot height	13.5mm
Winding turns/phase	300	Rotor shaft diameter	55mm
Rated current	15A	Rated speed	1000rpm

A. Rough Optimization

The goal of rough optimization is to sketch a rough design of the rotor structure. Rotor topology of a 4 flux barriers complete rotor [9] design is presented in Fig. 2. This design has flux barriers uniformly distributed and the rotor structure can be certain once flux barrier number, flux barriers width and position of flux barriers on q axis are defined. Set n_r as equivalent rotor slot per pole pair. Design angle θ_r of flux barriers can be calculated using equation (1).

$$\theta_r = \frac{2\pi}{pn_r} \tag{1}$$

where n_s as stator slot per pole pair and from article [10], condition $n_r = n_s \pm 4$ will gives minimum torque ripple. 3 or 4 flux barriers will give n_r in this range. The Fig. 3 shows the torque and torque ripple change from different flux barrier numbers. 4 is a suitable choice for the flux barrier number from the result. Rib1 and rib2's values are fixed at 1mm due to mechanical strength concern.

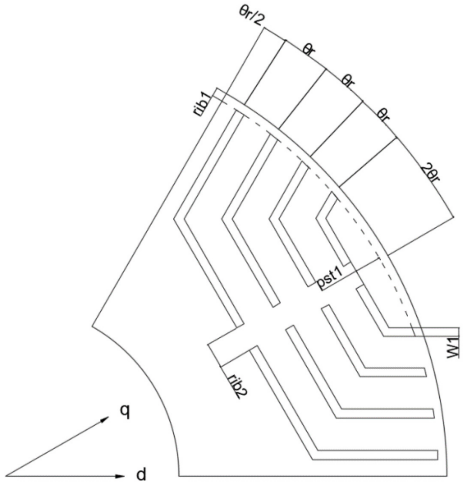

Fig 2. Rotor geometry of complete rotor (4 flux barriers).

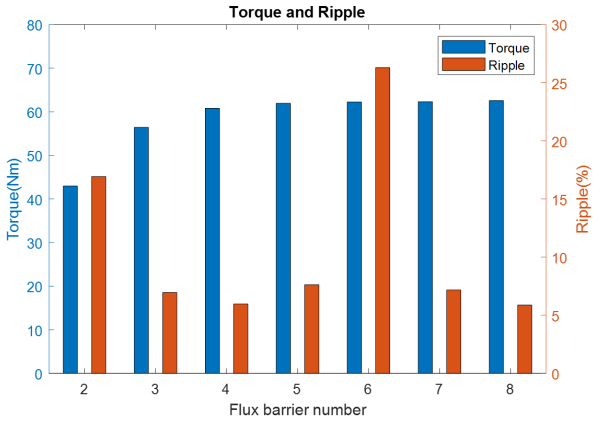

Fig 3. Average torque and torque ripple for different number of flux barriers.

After those above parameters are picked, only flux barriers' width and position of flux barriers on q axis are needed to certain the whole structure. Flux barrier ratio br and position p are picked for cross optimization and those parameters are defined using equation (2) and (3).

$$br = \frac{\sum w_{fluxbarrier}}{r_{rotor} - r_{shaft}} \tag{2}$$

$$p = \frac{pst}{r_{rotor} - r_{shaft}} \tag{3}$$

Set br's suitable range to be 0.25 to 0.75 with a step of 0.05, p's range to be 0 to 0.3 with a step of 0.02. 176 cases of different br and p pair is simulated, and the corresponding torque and torque ripple is shown in Fig. 4. From the result, br = 0.45 and p = 0,1 provides relatively maximum torque and minimum torque ripple.

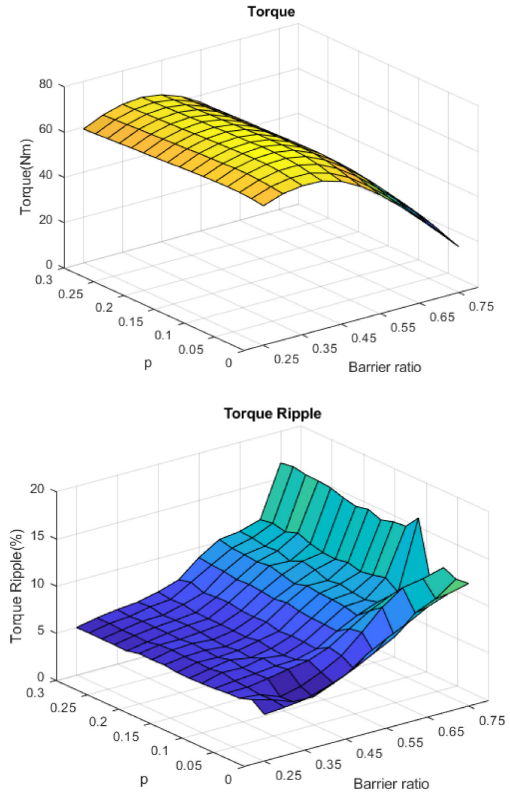

Fig 4. The influence of br and p values on average torque and torque ripple.

B. *Fine Optimization*

After rough optimization, rotor geometry is re-defined and all possible degrees of freedom are released. Since flux barriers are no longer uniformly distributed this time, it will need 4 parameters to restrict single flux barrier. Fig. 6 below shows 1st flux barrier's parameters under new geometry.

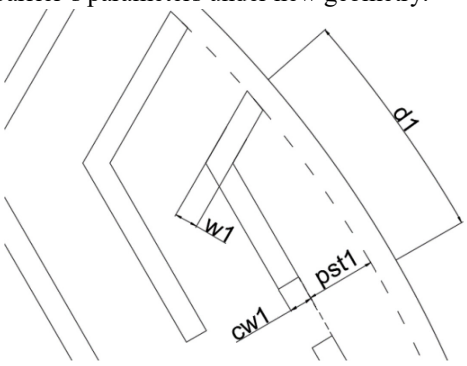

Fig 5. New rotor geometry of 1st flux barrier.

Total 16 parameters will be needed for the whole rotor structure, their initial value can be calculated from result of rough optimization. Detail parameters and their reference values are listed in Table II.

TABLE II
SPECIFIC PARAMETERS OF THE ROTOR

Parameter	reference value	Parameter	reference value
w1	3.01mm	d1	10.90°
w2	3.01mm	d2	16.36°
w3	3.01mm	d3	21.82°
w4	3.01mm	d4	27.27°
cw1	3.01mm	pst1	2.44mm
cw2	3.01mm	pst2	7.91mm
cw3	3.01mm	pst3	13.76mm
cw4	3.01mm	pst4	19.74mm

After setting reasonable test ranges, each parameter undergoes new simulations for new best value, if found, will replace old reference value. Take cw2 as an example, the result of its first and second iteration of fine optimization is shown in Fig. 6.

With old reference value of 3.01mm, first iteration of optimization tests cw2's values from 1 to 5mm. The results show that the overall rotor performance can be improved when cw2 is close to 2mm. Then 2mm will be assigned as new value for cw2 for this round of optimization. After all 16 parameters

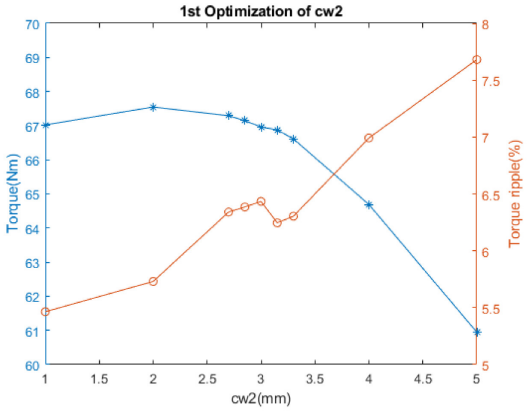

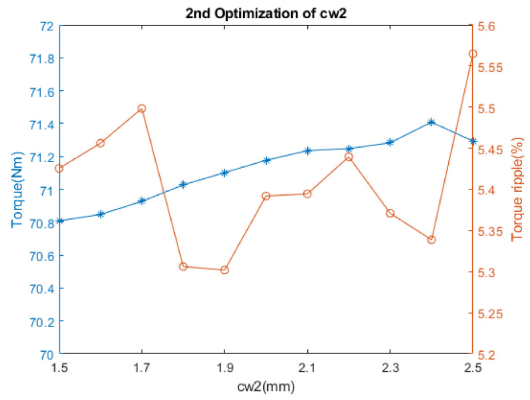

Fig 6. Torque and torque ripple change with respect to cw2 in first and second iteration.

have been optimized, a new round of optimization will take place for further squeeze the potential. For the same procedure, second iteration of optimization tests cw2's value from 1.5 to 2.5mm and finally decides the value of cw2 to be 2.4mm.

Since additional turns can have very limited improvement on performance, two iterations of optimization will be sufficient for this case. Final values of all 16 parameters after optimization are shown in Table III:

TABLE III
FINAL VALUE FOR PARAMETERS OF THE ROTOR

Parameter	reference value	Parameter	reference value
w1	3.01mm	d1	10.90°
w2	2.50mm	d2	16.36°
w3	2.50mm	d3	21.82°
w4	2.00mm	d4	27.27°
cw1	2.00mm	pst1	2.44mm
cw2	2.40mm	pst2	7.91mm
cw3	3.01mm	pst3	13.76mm
cw4	10.00mm	pst4	22.50mm

C. *Comparison of Results*

Fig. 7 below shows the specific rotor structure after rough optimization and after fine optimization.

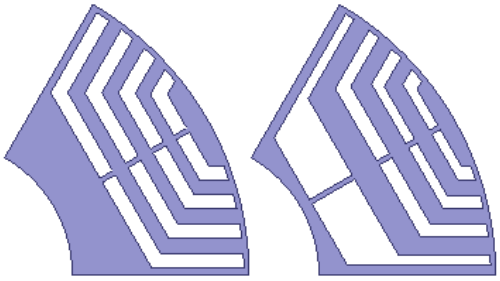

Fig 7. Rotor structure after rough and fine optimization.

The average torque improves from 67.12Nm to 71.20Nm after fine optimization. The average torque ripple improves from 6.63% to 5.35% after fine optimization. Overall performance improves about 6% from those data. It is proofed that the fine optimization can squeeze the potential of the structure a bit.

IV. PERFORMANCE EVALUATION

The Fig. 8 below shows the magnetic field on the whole structure. It can be seen that the structure has been magnetized properly. Those parts between rotor edge and flux barrier as well as parts on the flux bridge are highly magnetized to restrict the inductance on *q*-axis for a better performance of the SynRM.

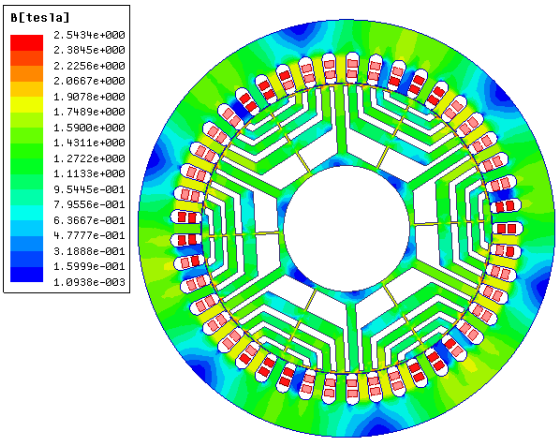

Fig 8. Flux density distribution of the stator and the rotor under rated current condition.

A. *Influence of the Current*

Change of the current will lead a change to the inductances on *q*-axis and *d*-axis and finally influence the torque produced.

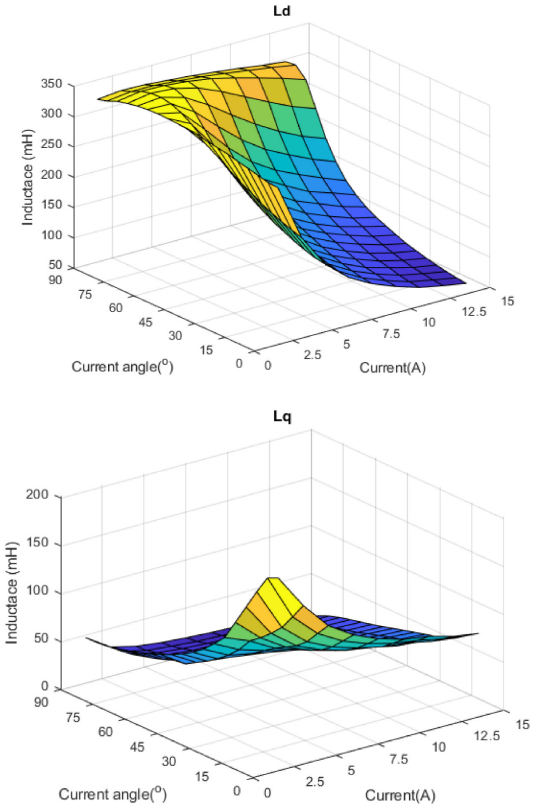

Fig 9. The inductance change on direct axis and quadratic axis.

Fig. 9 above shows the inductance change on direct axis and quadratic axis. Both the current amplitude and current phase angle has a great influence on inductances. Increasing current will lead a drop of the inductances on both axis. In addition, when the current angle approaching 90 deg (*q*-axis), the

influence of the current amplitude become smaller, and vice versa. The reason of this phenomenon is that the flux barrier locates on the *q*-axis and makes its inductance less influenced by the magnetic saturation.

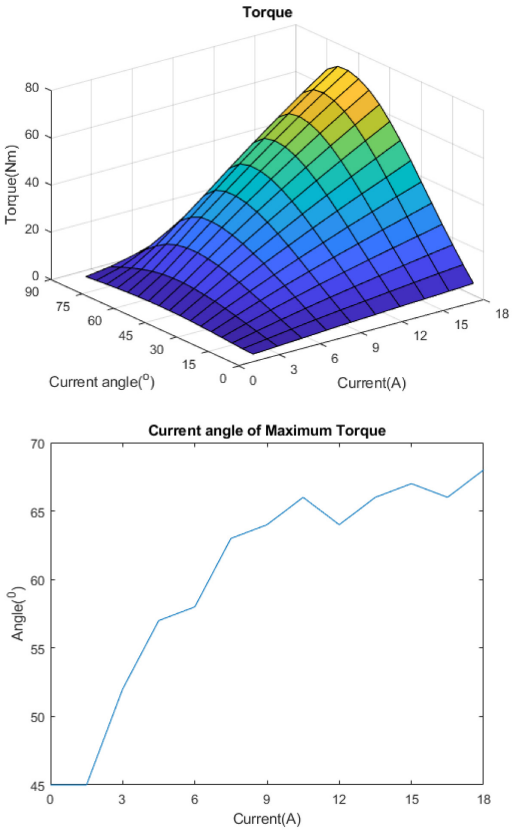

Fig 10. Torque change with different amplitude and current angle.

Fig. 10 shows the maximum torque varies with the current phase and the current amplitude. Generally, the torque increases when the amplitude of current increases. Function of electrical torque is defined using equation (4).

$$T_e = \frac{3}{2} P_n \left(\Psi_d i_q - \Psi_q i_d \right) = \frac{3}{2} P_n i_d i_q \left(L_d - L_q \right) \qquad (4)$$

Increasing in current amplitude will also increase the magnetization of the rotor and larger the current angle for maximum torque. The motor will have its maximum torque at 67deg current angle.

B. Performance at Rated Point

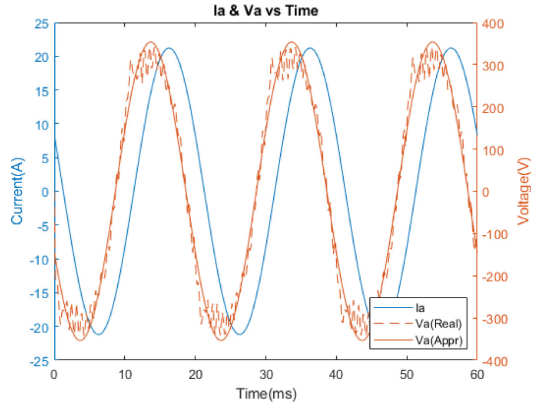

Fig 11. Current and Voltage at phase A winding.

Fig. 11 shows the waveform of voltage and current change at phase A winding. The solid line is the fitted sinusoid line of the voltage waveform. Current is lagging voltage for about 46 degrees.

Fig. 12 above shows the change of torque in one mechanic cycle. Average torque is 71.2Nm and the torque ripple is 5.35%.

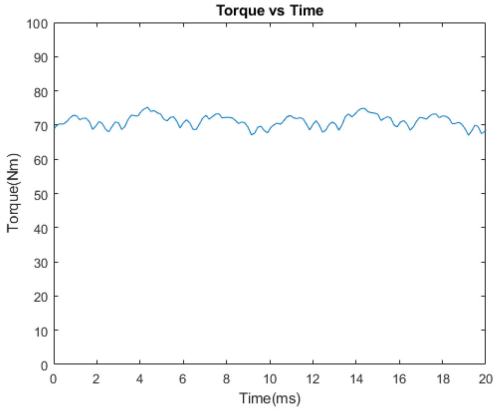

Fig 12. Electromagnetic Torque of SynRM.

Fig. 13 above shows the spectrum of torque waveform. Maximum torque ripple harmonic component is about 1.4% of the average torque. From the FEM model, the total core loss on stator and rotor is 40.38W and efficiency of the motor is calculated as 94.0%. Power factor is 0.71 which mean current is lagging the voltage of 45.14 deg, close to the result from measured waveforms.

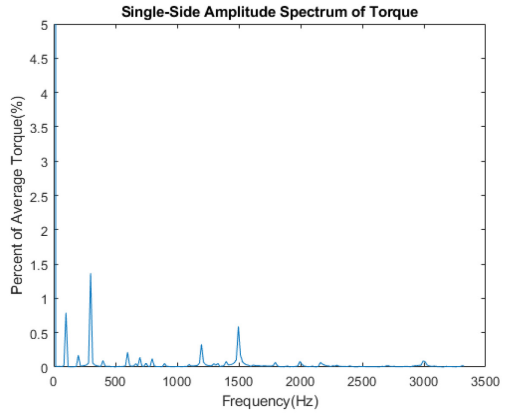

Fig 13. Spectrum of Torque waveform.

V. Conclusion

This paper summarized difference types of rotor geometry optimization approaches and introduce a compromise strategy to take consideration of both time saving and precision. Using torque and torque ripple and indicator, this paper optimized a rotor structure and tested its performance. The final result confirms the feasibility and efficiency of the new strategy.

References

[1] T. Matsuo and T. A. Lipo, "Rotor design optimization of synchronous reluctance machine", Energy Conversion, IEEE Transactions on, vol. 9, no. 2, pp. 359–365, 1994.

[2] T. A. Lipo, "Synchronous reluctance machines - a viable alternative for AC drives". *IEEE Electric Machines and Power Systems*. vol. 19

no. 6, pp. 659-671, 1991.

[3] D. A. Staton, T. J. E. Miller, and S.E. Wood, "Maximizing the Saliency Ratio of the Synchronous Reluctance Motor", *IEEE Proceedings on Electric Power Applications*, vol. 140, no. 4, pp. 249-259, 1993.

[4] Kolehmainen J, "Synchronous Reluctance Motor with Form Blocked Rotor", Energy Conversion, *IEEE Transactions on Energy Conversion*, col. 25, no, 2, pp. 450-456, 2010.

[5] H. Kiriyama, S. Kawano, Y. Honda, et a1, "High Performance Synchronous Reluctance Motor with Multi-flux Barrier for the Appliance Industry", *in Proc. IEEE Industry Applications Conference*. 1998, pp. 111·117.

[6] K. Wang, Z. Zhu, G. Ombach, M. Koch, S. Zhang, and J. Xu, "Optimal slot/pole and flux-barrier layer number combinations for synchronous reluctance machines," in *Proc. Ecological Vehicles and Renewable Energies (EVER), 2013 8th International Conference and Exhibition on. IEEE*, 2013, pp. 1–8.

[7] C. Babetto, G. Bacco and N. Bianchi, "Synchronous Reluctance Machine Optimization for High Speed Applications", *IEEE Transactions on Energy Conversion.* 2018 DOI 10.1109

[8] S. Orlova, A. Vezzini, and V. Pugachov, "Analysis of Parameters for optimal design of Synchronous Reluctance Motor", in 56th International Scientific Conference on Power and Electrical Engineering of Riga Technical University (RTUCON), Oct 14th 2015

[9] Moghaddam R R, Magnussen F, Sadarangani C. Novel Rotor Design Optimization of Synchronous Reluctance Machine for High Torque Density [J]. IET International Conference on Power Electronics, 2012, 592: 32.

[10] B. Boazzo, A. Vagati, G. Pellegrino, E. Armando, and P. Guglielmi, "Multipolar ferrite-assisted synchronous reluctance machines: A general design approach," *IEEE Transactions on Industrial Electronics*, vol. 62, no. 2, pp. 832–845, 2015.

[11] A. Vagati, M. Pastorelli, G. Franceschini, and S. C. Petrache, "Design of low-torque-ripple Synchronous Reluctance motors", IEEE Transactions on Industry Applications", vol. 34, no. 4, pp. 758-765, July./Aug. 1998

Ken Chen received the B.S. degree in Electrical Engineering from Purdue University, West Lafayette, USA, in 2017 and currently working toward M.S. degree in Electrical Engineering in Ming Hsieh Department of Electrical engineering, University of Southern California, Los Angeles, USA.

His current research interest in synchronous reluctance motor parameter estimation and structure optimization.

Wenfei Yu received the M.S. degree in electric machines at Zhengzhou University of Light Industry, Zhengzhou, China, in 2018. Since 2018, he has been working toward the Ph.D. degree in the School of Electric Engineering, Southeast University, Nanjing, China.

His current research interests include electromagnetic and thermal analysis on electrical machines, particularly on permanent magnetic machines.

Chuanxin Wen received the M.S. Degrees in Electrical engineering from Southeast University, Nanjing, China, in 2004. Since 2004, he has been with NARI Group Corporation, where he is currently a manager of electric vehicle drive system.

His main research directions include power electronic converter control technology and high-efficiency control technology for electric vehicle drive motors.